Journal of Power Sources 195 (2010) 1854–1858

Contents lists available at ScienceDirect

Journal of Power Sources

journal homepage: www.elsevier.com/locate/jpowsour

Short communication

$La_{1-x}Sr_xCoO_3$ ($x = 0.1–0.5$) as the cathode catalyst for a direct borohydride fuel cell

Yan Liu, Yongning Liu*, Jinfu Ma, Junhua Lai

State Key Laboratory for Mechanical Behavior of Materials, Xi'an Jiaotong University, Xi'an 710049, PR China

ARTICLE INFO

Article history:
Received 11 August 2009
Received in revised form
22 September 2009
Accepted 6 October 2009
Available online 18 November 2009

Keywords:
Direct borohydride fuel cell
$La_{1-x}Sr_xCoO_3$
Hydrogen storage alloy
Cell performance

ABSTRACT

Direct borohydride fuel cells (DBFCs), with a series of perovskite-type oxides $La_{1-x}Sr_xCoO_3$ ($x = 0.1–0.5$) as the cathode catalysts and a hydrogen storage alloy as the anode catalyst, are studied in this paper. The structures of the perovskite-type catalysts are mainly $La_{1-x}Sr_xCoO_3$ ($x = 0.1–0.5$) oxides phases. However, with the increase of strontium content, the intensities of the X-ray diffraction peaks of the impure phases $La_2Sr_2O_5$ and $SrLaCoO_4$ are gradually enhanced. Without using any precious metals or expensive ion exchange membranes, a maximum current density of 275 mA cm^{-2} and a power density of 109 mW cm^{-2} are obtained with the Sr content of $x = 0.2$ at 60 °C for this novel type of fuel cell.

1. Introduction

The direct borohydride fuel cell (DBFC) has attracted much attention [1–7] due to its high theoretical open cell voltage (OCV) of 1.64 V, its excellent hydrogen capacity of 9.3 kWh kg^{-1} ($NaBH_4$) and the possibility of using non-precious metal catalysts for both the cathode and the anode [8–10].

In recent years, many studies have been carried out on the cathode catalyst of DBFCs [11–17]. The use of Ag [6,11] and MnO_2 [9,12,13] has been reported. However, poor stability and weak resistance greatly limited the cell performances [6]. A cobalt polypyrrole carbon (Co-PPY-C) composite was researched as a cathode catalyst, but a precious metal ion exchange membrane was used [14]. A DBFC of polypyrrole modified carbon-supported cobalt hydroxide ($Co(OH)_2$-PPY-C)[15] showed good cell performance, achieving a maximum power density of 83 mW cm^{-2}. In previous works, we have shown that cobalt phthalocyanine (CoPc) [16] and iron phthalocyanine (FePc) [17] exhibited good catalytic activity for the oxygen reduction reaction (ORR) and good borohydride tolerance, and thus they are expected to be alternatives to the noble metal Pt as the cathode catalyst. In terms of their high conductivity and outstanding catalytic activity and stability in alkaline media, perovskite oxides (ABO_3) [18,19] have recently attracted interest. However, very little progress has been achieved on the reduction activities of the perovskite-type oxides in DBFCs. Therefore, it is significant to attempt to use perovskite-type oxides as electronic conductors and catalysts for the ORR in DBFCs.

This paper reports the use of perovskite-type oxides, $La_{1-x}Sr_xCoO_3$ ($x = 0.1–0.5$) with Sr substitution for La, as the cathode catalysts for DBFCs. A hydrogen storage alloy (HSA) is used as the anodic catalyst, which could alleviate the low utilization of the BH_4^- ions arising from the BH_4^- decomposition reaction on the anode. The effects of Sr content on the microstructure and electrochemical catalytic activity were investigated in detail.

2. Experimental

2.1. Materials and characterization

$La_{1-x}Sr_xCoO_3$ ($x = 0.1–0.5$) perovskite oxides were prepared by a sol–gel method [20]. Lanthanum nitrate ($La(NO_3)_3{\cdot}6H_2O$), strontium nitrate ($Sr(NO_3)$), cobalt nitrate ($Co(NO_3)_2{\cdot}6H_2O$), citric acid ($C_6H_8O_7{\cdot}H_2O$) and ammonium hydroxide (NH_4OH) were used as the raw materials, all of analytical grade purity. According to the stoichiometric composition of the reactants, specified amounts of $La(NO_3)_3{\cdot}6H_2O$, $Co(NO_3)_2{\cdot}6H_2O$ and $Sr(NO_3)_2$ were first dissolved in deionized water, and then a specific amount of $C_6H_8O_7{\cdot}H_2O$ was added to the solution. The amount of molar $C_6H_8O_7{\cdot}H_2O$ was equal to that of the metal nitrates in the solution. NH_4OH was slowly added to adjust the pH value of the solution in the range of 6–7 to stabilize the nitrate–citrate solution. During this procedure, the solution was kept at a temperature of 70 °C and continuously stirred until a deep-red gel was obtained; the precursor was produced from a subsequent drying process in a vacuum at 80 °C. Furthermore, the gel was heated until spontaneous combustion occurred, and the

* Corresponding author. Tel.: +86 29 8266 4602; fax: +86 29 8266 3453.
E-mail address: ynliu@mail.xjtu.edu.cn (Y. Liu).

0378-7753/$ – see front matter © 2009 Elsevier B.V. All rights reserved.
doi:10.1016/j.jpowsour.2009.10.016

gel burnt up rapidly. Then the loose precursor powder was ground. Finally, the ground powder was calcined at 800 °C for 2 h in air in order to form $La_{1-x}Sr_xCoO_3$ (x = 0.1–0.5).

The crystalline structure of the $La_{1-x}Sr_xCoO_3$ (x = 0.1–0.5) powder was investigated with an X-ray diffractometer (D/MAX-3A, Japan) using CuKα radiation (k = 0.154056 nm). Specific surface area and porosity analyzer (ASAP2020, Mack Instrument Company, USA) was employed to study the BET surface area of the selected catalysts $La_{1-x}Sr_xCoO_3$ (x = 0.2–0.4).

The anode catalyst, $MmNi_{3.55}Co_{0.75}Mn_{0.4}Al_{0.3}$ (where Mm denotes Ce-rich mixed mischmetal composed of 50 wt.% Ce, 30 wt.% La, 5 wt.% Pr and 15 wt.% Nd) alloy, was prepared by inductive melting under an argon atmosphere, and then mechanically crashed into powder smaller than 100 μm. The purity of all additive elements was over 99.9 wt.%.

2.2. Electrode preparation

The cathode electrode used in this system was a three-layer electrode consisting of a gas diffusion layer, an active layer, and a current accumulating matrix. The active layer was prepared by mechanically mixing 30 wt.% $La_xSr_{1-x}CoO_3$ (x = 0.1–0.5) and 45 wt.% activated carbon and then adding 25 wt.% polytetrafluoroethylene (PTFE) (solid quality) to the floured powder. Next, the powder mixture was pasted onto a Ni foam (thickness = 1.7 mm, porosity >95%). The gas diffusion layer was prepared by mixing 60 wt.% acetylene black and 40 wt.% PTFE (solid quality) with ethanol into a 0.3 mm thick film. Then the prepared diffusion layer was heated at 340 °C for 1 h. The three-layer gas electrode was finished by pressing the coated Ni foam and the gas diffusion layer into a 0.6 mm thick sheet at 120 kgf cm^{-2}.

The hydrogen storage alloy, $MmNi_{3.55}Co_{0.75}Mn_{0.4}Al_{0.3}$ alloy powder (95 wt.%), was used as the anode electrode material. Acetylene black (2 wt.%) and cobalt monoxide (3 wt.%) were also added to improve the electrochemical activity and the high-rate discharge ability of the alloy electrode. Then the mixture was pasted onto a Ni foam (thickness = 1.7 mm, porosity >95%). After drying at 80 °C in a vacuum for 2 h, the catalyst layer was pressed at 120 kgf cm^{-2}. Before testing, the anode was pretreated in a 6 M KOH and 0.8 M KBH_4 aqueous solution for 24 h for activation. The mass loadings of $La_xSr_{1-x}CoO_3$ in the cathode and hydrogen storage alloy in the anode were 7.5 mg cm^{-2} and 150 mg cm^{-2}, respectively.

2.3. Electrochemical measurements

2.3.1. Half-cell tests

Line sweep voltammetry (LSV) was employed to characterize the electrochemical performance of the cathode using a computer controlled Electrochemistry Workstation CHI600 (Chenhua, Shanghai, China) with a conventional three-electrode configuration seen in Fig. 1. The cathode served as the working electrodes. A Hg/HgO/6 M KOH electrode was used as a reference electrode, and a Pt wire as a counter electrode for polarization measurements. Fig. 1 shows the cathode three-electrode test system, a cathode was placed on a window on one side of the square container, whose active area was 1 cm^2. The reference electrode was placed in a Luggin capillary with its tip positioned close to the working electrode. Distance between counter electrode (Pt wire) and working electrode was 1 cm. The space among the three electrodes was used to feed with the fresh electrolyte (KOH) through a pump. The scan rate is 5 mV s^{-1}.

2.3.2. Single-cell tests

The discharging properties and battery life of the single DBFC cell was measured by a battery testing system (from Neware Technology Limited, Shenzhen, China). Fig. 2 shows the cell system. The

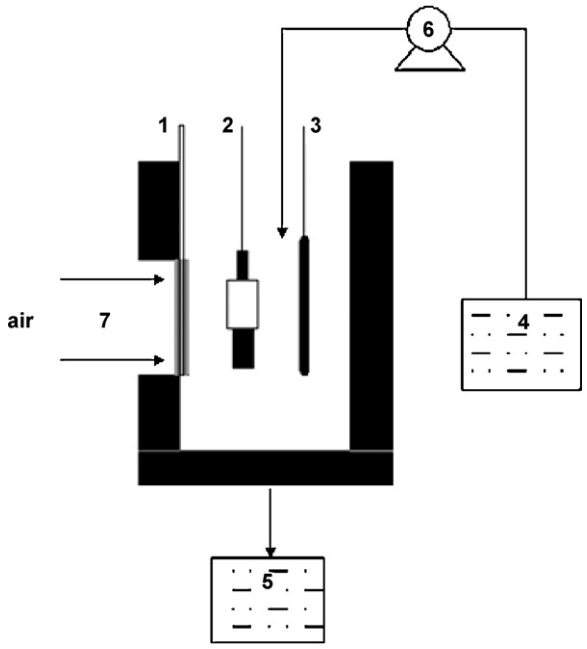

Fig. 1. Schematic diagram of cathode three-electrode test system: (1) cathode; (2) reference electrode (Hg/HgO); (3) counter electrode (Pt wire); (4) fresh fuel–electrolyte mixture storage; (5) exhausted fuel–electrolyte mixture storage; (6) pump; and (7) air.

cathode was placed on one side of the square container, the gas diffusion layer was exposed to air and the active layer was contacted with the electrolyte, an anode was placed on the other side with a gap of 1 cm between the two electrodes. The space of the two electrodes was used to feed with the fresh mixture of electrolyte (6 M KOH) and fuel (0.8 M KBH_4) through a pump.

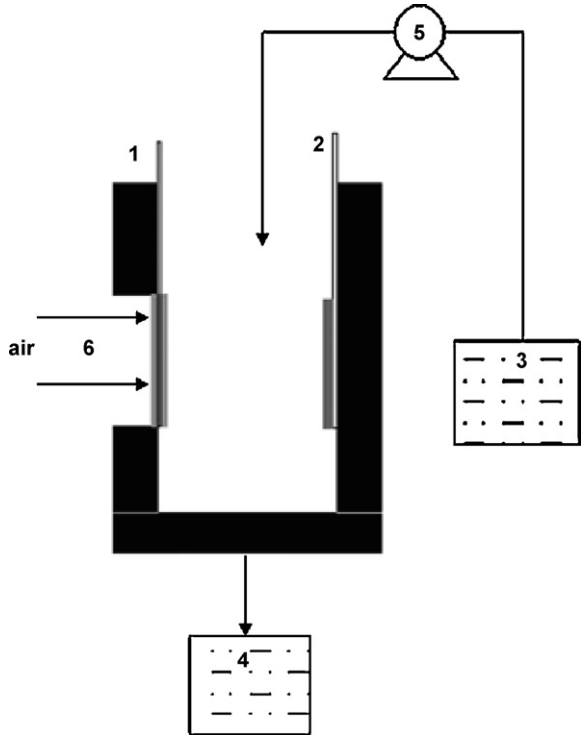

Fig. 2. Schematic diagram of air-breathing DBFC: (1) cathode; (2) anode; (3) fresh fuel–electrolyte mixture storage; (4) exhausted fuel–electrolyte mixture storage; (5) pump; and (6) air.

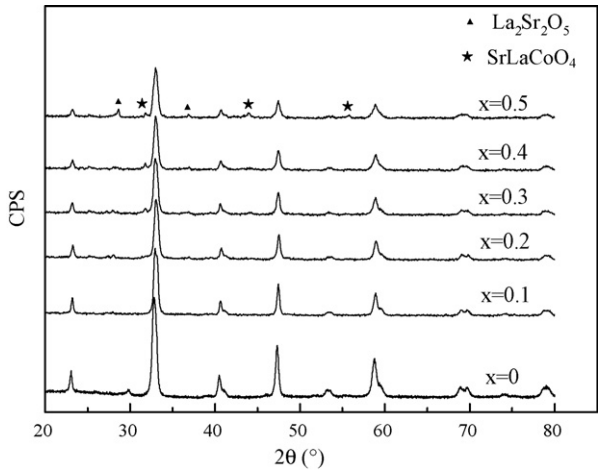

Fig. 3. XRD patterns of the series of perovskite-type oxides $La_{1-x}Sr_xCoO_3$ (x = 0–0.5).

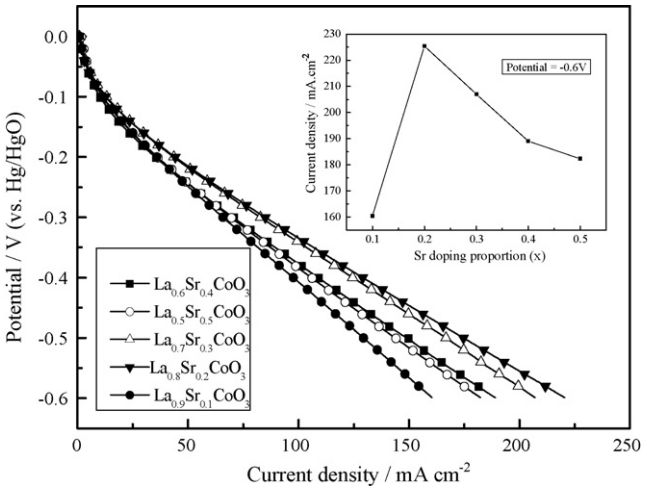

Fig. 4. Half-cell test: the polarization curves of $La_{1-x}Sr_xCoO_3$ (x = 0–0.5) for different Sr contents. Electrolyte: 6 M KOH. Scan rate: 5 mV s^{-1}. Operation temperature: 25 °C.

Table 1
Average crystal sizes of catalysts.

Catalysts	Dc (nm)
$La_{0.9}Sr_{0.1}CoO_3$	27.52206
$La_{0.8}Sr_{0.2}CoO_3$	25.30822
$La_{0.7}Sr_{0.3}CoO_3$	24.30299
$La_{0.6}Sr_{0.4}CoO_3$	22.82702
$La_{0.5}Sr_{0.5}CoO_3$	22.17338

3. Results and discussion

3.1. Characterization of $La_{1-x}Sr_xCoO_3$n (x = 0–0.5)

Fig. 3 shows the XRD patterns of a series of perovskite-type oxides $La_{1-x}Sr_xCoO_3$ (x = 0–0.5). As shown in Fig. 3, catalysts with different Sr concentrations all exhibit perovskite-type phase diffraction patterns. When the content Sr is higher than 0.1, strontium lanthanum oxide $La_2Sr_2O_5$ (2θ = 28.681°, 36.868°) impure peaks are observed. And with the higher amount of Sr content x = 0.3, strontium lanthanum cobalt oxide $SrLaCoO_4$ (2θ = 31.731°, 44.266°, 56.499°) impure peaks also can be observed. With increasing Sr substitution, the intensity of the characteristic diffraction peaks for the perovskite-type phase gradually weakens, while the intensity of the characteristic diffraction peaks for the impure peaks $La_2Sr_2O_5$ and $SrLaCoO_4$ is gradually enhanced. The results of the XRD patterns show that not all Sr^{2+} enters the crystalline lattice of the perovskite-type phase, and some ions form impure phases, which may lead to the formation of the lattice defects of the $La_{1-x}Sr_xCoO_3$ perovskite-type phase.

Table 1 gives the average crystal sizes of catalysts. Based on the XRD results and the Scherer formula: $Dc = k\lambda/\beta\cos\theta$ (k is the Scherer constant, λ is the wavelength of the X-ray, here it is 0.154056, β is half-peak width (FWHM), θ is the diffraction angle.) we calculated the average crystal sizes of catalysts. As can be seen from Table 1, the catalysts prepared are all among the range of the nano meter and the difference of crystal sizes is very little.

Table 2 shows BET surface areas of the three catalysts. Three samples have been selected, $La_{1-x}Sr_xCoO_3$ (x = 0.2, 0.3, 0.4). As can be seen from Table 2, the perovskite catalyst $La_{0.8}Sr_{0.2}CoO_3$ has higher surface areas 17.1476 $m^2\ g^{-1}$ compared with the other two samples. However, there is no obvious difference about the BET surface areas among the three samples.

Table 2
Measured BET surface areas of three catalysts.

Catalysts	BET ($m^2\ g^{-1}$)
$La_{0.8}Sr_{0.2}CoO_3$	17.1476
$La_{0.7}Sr_{0.3}CoO_3$	16.0498
$La_{0.6}Sr_{0.4}CoO_3$	14.3091

3.2. Influence of Sr content on cathode properties

Fig. 4 gives the polarization curves for the $La_{1-x}Sr_xCoO_3$ (x = 0.1–0.5) catalyzed cathodes with different Sr contents. With increasing Sr ratio, the polarization of the cathodes decreases first and then increases. The current densities of the $La_{1-x}Sr_xCoO_3$-catalyzed cathode are ordered from large to small as $La_{0.8}Sr_{0.2}CoO_3 > La_{0.7}Sr_{0.3}CoO_3 > La_{0.6}Sr_{0.4}CoO_3 > La_{0.5}Sr_{0.5}CoO_3 > La_{0.9}Sr_{0.1}CoO_3$. When the Sr content is 0.2, the polarization has a minimum, and a current density of 225 mA cm^{-2} is obtained. To fully explain the observed activities is really not very easy. It is generally accepted that some relatively lattice defect leading to the labile oxygen species are the main active sites [21–24]. However, the impure phases also may influence the activity of the catalysts. For each composition, some cooperation between the second phases and the lattice defect could occur. At first, the activity is significantly enhanced due to the formation of the defective perovskite phase with the oxygen mobility higher than in $La_{0.9}Sr_{0.1}CoO_3$. As the amount of Sr substitution increases, apparent activity is influenced by the gradual formation of additional phases. When x = 0.2, the amount of segregated the strontium lanthanum oxide $La_2Sr_2O_5$ is less and its effect is small. When x larger than 0.3, a larger amount of segregated strontium lanthanum cobalt oxide $SrLaCoO_4$ also appears along with a increase of the strontium lanthanum oxide $La_2Sr_2O_5$. The diminution of activity might be considered as the cooperation of the lattice defect and the second phases. The higher amount of the second phases may destroy the perovskite structure, which may lead the activity diminution of the catalyst.

3.3. Performance of a $La_{0.8}Sr_{0.2}CoO_3$-catalyzed cathode at different operating temperatures

As shown in Fig. 5, a $La_{0.8}Sr_{0.2}CoO_3$-catalyzed cathode at different operating temperatures was studied. As the temperature increases from 25 °C to 60 °C, the cathode polarization gradually decreases. The cutoff current density shifts from 225 mA cm^{-2} to 275 mA cm^{-2}, which may be attributed to the increase in the conductivity of the electrolyte solution. This study confirms that the catalyst we prepared could work over a relative wide tempera-

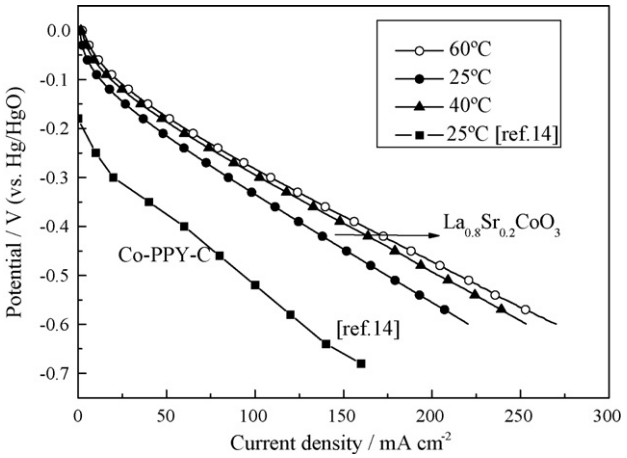

Fig. 5. Half-cell test: performances of a $La_{0.8}Sr_{0.2}CoO_3$-catalyzed cathode at different operating temperatures. Scan rate: 5 mV s^{-1}.

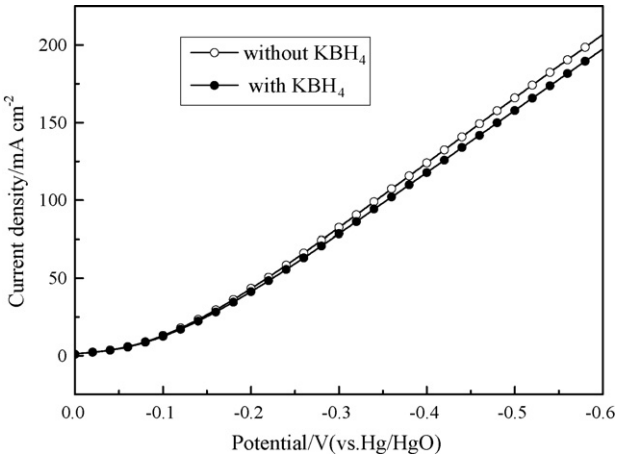

Fig. 7. The polarization curves of a $La_{0.8}Sr_{0.2}CoO_3$-catalyzed air cathode in 6 M KOH solution with or without the addition of 0.8 M KBH_4. Scan rate: 5 mV s^{-1}. Operation temperature: 25 °C.

ture range. Fig. 5 also shows the polarization curve of a cobalt polypyrrole composite (CO-PPY-C)-catalyzed cathode reported in a reference [14]. As shown in Fig. 5, the polarization of this cathode is serious, and the current density is about 140 mA cm^{-2} at a potential of −0.6 V at 25 °C. In comparison, the ending current density of the $La_{0.8}Sr_{0.2}CoO_3$-catalyzed cathode is 225 mA cm^{-2} under the same conditions, suggesting that the $La_{0.8}Sr_{0.2}CoO_3$ cathode has better electrochemical performance.

3.4. Performance of the cell at different operating temperatures

As presented in Fig. 6, the influence of temperature on the performance of DBFCs is quite obvious. The peak power density is significantly enhanced by increasing the operating temperature. The maximum power densities obtained are 83 mW cm^{-2}, 89 mW cm^{-2}, and 109 mW cm^{-2} at 25 °C, 40 °C, and 60 °C, respectively. The reason for this phenomenon may be the increase in the diffusion coefficient and the increase in the mass transfer of the reactants. Meanwhile, the voltage and the current at the steady-state of the polarization curve almost have a linear relationship, suggesting that there are no obviously activation or concentration polarizations, except for ohmic polarization. In addition, the peak power density is higher than those of MnO_2 [9] and Co-PPY-C catalyzed cathodes [14] at 25 °C.

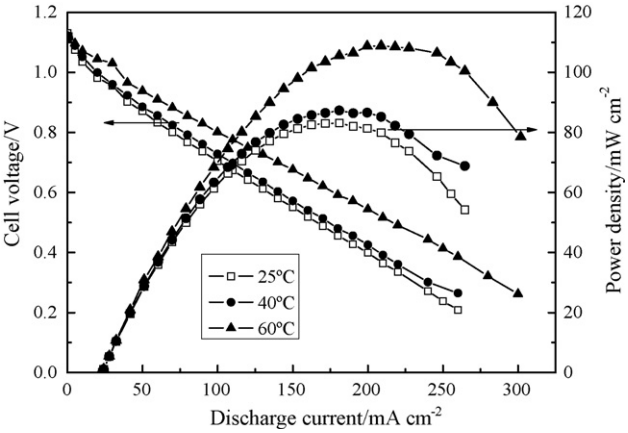

Fig. 6. The influence of temperature on the performance of a DBFC based on a $La_{0.8}Sr_{0.2}CoO_3$ cathode and AB_5 alloy anode. Electrolyte: 6 M KOH + 0.8 M KBH_4.

3.5. Tolerance

Whether the precious ion exchange membrane should be used in the cell depends on the tolerance for borohydride of the cathode. Fig. 7 exhibits the polarization curves of the $La_{0.8}Sr_{0.2}CoO_3$-catalyzed cathode in 6 M KOH solutions with or without the addition of 0.8 M KBH_4. The two curves almost coincide at low potential. With increasing potential, a small derivation is observed. However, overall, the polarization curve of the $La_{0.8}Sr_{0.2}CoO_3$-catalyzed cathode in the presence of BH_4^- ions is approximately identical to that in the absence BH_4^- ions, indicating that the existence of BH_4^- ions has no serious harmful effect on the discharge performance of the cathode. This result confirms that in this DBFC a membraneless structure could be designed.

3.6. Stability of the cell

The cell stability was tested by monitoring changes in cell voltage during galvanostatic operation. Fig. 8 shows the changes of the cell voltage at a constant current discharge of 20 mA cm^{-2} over a period of 60 h at ambient atmosphere. As shown in Fig. 8, although some tiny change in the cell voltage is observed, no degradation occurs, suggesting that the cell has good durability over the test

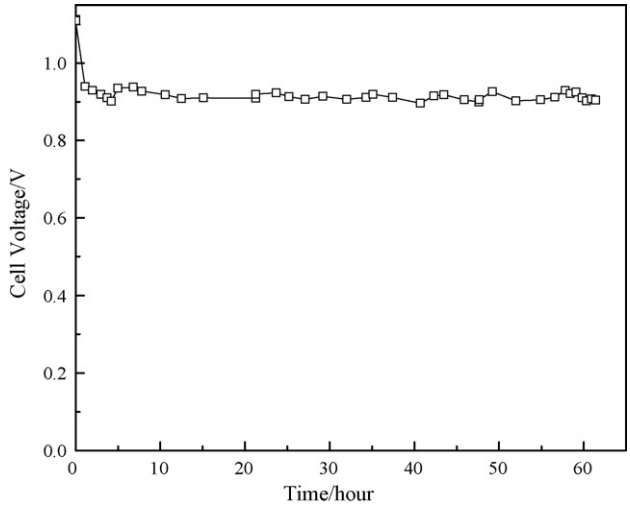

Fig. 8. Stability test of the DBFC using a $La_{0.8}Sr_{0.2}CoO_3$ cathode. Operation at a current density of 20 mA cm^{-2} at ambient conditions.

period. In addition, the open circuit voltage (OCV) of the cell (1.11 V) is much higher than those of DBFCs with Pt and Ag catalysts in reference [11]. In addition, the cell performance stability was improved when using the $La_{0.8}Sr_{0.2}CoO_3$-catalyzed cathode compared with the DBFCs with Pt and Ag catalysts.

4. Conclusions

In this study, $La_xSr_{1-x}CoO_3$ ($x = 0.1$–0.5) was investigated as the cathodic catalyst of a DBFC. A maximum power density of 109 mW cm^{-2} and current density of 275 mA cm^{-2} were achieved at 60 °C with the catalyst $La_{0.8}Sr_{0.2}CoO_3$ as the cathode. Due to the good tolerance for borohydride of the $La_{0.8}Sr_{0.2}CoO_3$-catalyzed cathode, the cell was designed without using any expensive ion exchange membrane. In addition, it was found that the cell had good short-term durability with the $La_{0.8}Sr_{0.2}CoO_3$-catalyzed cathode.

References

[1] C. Ponce de Leon, F.C. Walsh, D. Pletcher, D.J. Browning, J.B. Lakeman, J. Power Sources 155 (2006) 172–181.
[2] J.H. Wee, J. Power Sources 161 (2006) 1–10.
[3] U.B. Demirci, J. Power Sources 169 (2007) 239–246.
[4] N.A. Choudhury, R.K. Raman, S. Sampath, A.K. Shukla, J. Power Sources 143 (2005) 1–8.
[5] Z.P. Li, B.H. Liu, K. Arai, S. Suda, J. Alloys Compd. 404–406 (2005) 648–652.
[6] H. Cheng, K. Scott, K. Lovell, Fuel Cells 6 (2006) 367–375.
[7] A. Verma, S. Basu, J. Power Sources 145 (2005) 282–285.
[8] H. Cheng, K. Scott, J. Electroanal. Chem. 596 (2006) 117–123.
[9] Y.G. Wang, Y.Y. Xia, Electrochem. Commun. 8 (2006) 1775–1778.
[10] B.H. Liu, S. Suda, J. Alloys Compd. 454 (2008) 280–285.
[11] B.H. Liu, S. Suda, J. Power Sources 164 (2007) 100–104.
[12] R.X. Feng, H. Dong, Y.D. Wang, X.P. Ai, Y.L. Cao, H.X. Yang, Electrochem. Commun. 7 (2005) 449–452.
[13] A. Verma, A.K. Jha, S. Basu, J. Power Sources 141 (2005) 30–34.
[14] H.Y. Qin, Z.X. Liu, W.X. Yin, J.K. Zhu, Z.P. Li, J. Power Sources 185 (2008) 909–912.
[15] H.Y. Qin, Z.X. Liu, L.Q. Ye, J.K. Zhu, Z.P. Li, J. Power Sources 192 (2009) 385–390.
[16] J.F. Ma, Y.N. Liu, P. Zhang, J. Wang, Electrochem. Commun. 10 (2008) 100–102.
[17] J.F. Ma, J. Wang, Y.N. Liu, J. Power Sources 172 (2007) 220–224.
[18] P. Datta, P. Majewski, F. Aldinger, J. Eur. Ceram. Soc. 29 (2009) 1469–1476.
[19] J.F. Ma, Y.N. Liu, Y. Liu, Y.S. Yan, P. Zhang, Fuel cells 8 (2008) 394–398.
[20] Z. Yang, Y. Huang, B. Dong, H.L. Li, J. Solid State Chem. 178 (2005) 1157–1164.
[21] Jitka Kirchnerova1, Mihai Alifanti, Bernard Delmon, Appl. Catal. A: Gen. 231 (2002) 65–80.
[22] Z.J. Qu, C.Y. Yu, W.Z. Li, Y.X. Chen, Acta Physico-chim. Sinica 10 (1994) 796–801.
[23] G.I. Golodets, Heterogeneous Catalytic Reactions Involving Molecular Oxygen, Studies in Surface Science and Catalysis, vol. 15, Elsevier, Amsterdam, 1983, pp. 437–469.
[24] A. Bielanski, J. Haber, Catal. Rev., Sci. Eng. 19 (1979) 1–41.